 Related Commentary, page 1849

# Epididymis seleno-independent glutathione peroxidase 5 maintains sperm DNA integrity in mice

Eléonore Chabory,[1] Christelle Damon,[1] Alain Lenoir,[1] Gary Kauselmann,[2] Hedrun Kern,[2] Branko Zevnik,[2] Catherine Garrel,[3] Fabrice Saez,[1] Rémi Cadet,[1] Joelle Henry-Berger,[1] Michael Schoor,[2] Ulrich Gottwald,[4] Ursula Habenicht,[4] Joël R. Drevet,[1] and Patrick Vernet[1]

[1]"Epididymis & Sperm Maturation", GReD, CNRS UMR 6247, INSERM U931, Clermont Université, Aubière, France. [2]TaconicArtemis GmbH, Cologne, Germany. [3]Laboratoire de Biologie du Stress Oxydant, Département de Biologie Intégrée, CHU de Grenoble, Grenoble, France. [4]TRG Gynecology & Andrology and Male Health Care Research, Bayer Schering Pharma AG, Berlin, Germany.

**The mammalian epididymis provides sperm with an environment that promotes their maturation and protects them from external stresses. For example, it harbors an array of antioxidants, including non-conventional glutathione peroxidase 5 (GPX5), to protect them from oxidative stress. To explore the role of GPX5 in the epididymis, we generated mice that lack epididymal expression of the enzyme. Histological analyses of *Gpx5*$^{-/-}$ epididymides and sperm cells revealed no obvious defects. Furthermore, there were no apparent differences in the fertilization rate of sexually mature *Gpx5*$^{-/-}$ male mice compared with WT male mice. However, a higher incidence of miscarriages and developmental defects were observed when WT female mice were mated with Gpx5-deficient males over 1 year old compared with WT males of the same age. Flow cytometric analysis of spermatozoa recovered from *Gpx5*-null and WT male mice revealed that sperm DNA compaction was substantially lower in the cauda epididymides of *Gpx5*-null animals and that they suffered from DNA oxidative attacks. Real-time PCR analysis of enzymatic scavengers expressed in the mouse epididymis indicated that the cauda epididymidis epithelium of *Gpx5*-null male mice mounted an antioxidant response to cope with an excess of ROS. These observations suggest that GPX5 is a potent antioxidant scavenger in the luminal compartment of the mouse cauda epididymidis that protects spermatozoa from oxidative injuries that could compromise their integrity and, consequently, embryo viability.**

## Introduction

In mammals, epididymis transit appears to be an essential step for sperm cells to fully develop their fertilizing abilities. When they leave the testis and enter the epididymis, spermatozoa have developed their highly differentiated morphology but are still functionally immature in the sense that they cannot recognize, bind to, and penetrate oocytes. Being transcriptionally and translationally silent, spermatozoa progressively acquire their fertilizing potential during epididymal descent, relying on the activities of the epididymis epithelium that creates an ever-changing luminal environment along the duct. The sequential character of the various secretory and reabsorption activities of the epididymis epithelium *in fine* leads to extensive modifications, essentially but not exclusively, of the sperm plasma membrane. Modifications concern qualitative and quantitative presence of proteins but also of their sugar moieties and membranous lipids (1).

In addition to the preparation of sperm cells for fertilization, the epididymis is responsible for protection and survival of spermatozoa during their epididymal journey and also during storage between 2 ejaculations, in the distal part of the organ (the cauda). This protection is critical because spermatozoa are particularly vulnerable cells devoid of any ability to elicit classic defense responses when challenged. The absence of cytoplasmic material and, consequently, of the various protective enzymatic activities that it contains, together with their haploid state and the highly compacted nature of their DNA explain this situation. Among the stresses that sperm cells have to cope with is oxidative stress. Due to the unusual composition of their plasma membrane, very rich in polyunsaturated fatty acids, one major threat for sperm cells is oxidative damage (2). Much evidence has shown that sperm cells and male fertility are impaired by oxidative stress, whether it is due to a lack of antioxidant protection or to excess in ROS generation (reviewed in ref. 3). In support of sperm susceptibility to ROS-mediated damages, we and others have shown that the mammalian epididymis provides an extensive array of both enzymatic and non-enzymatic antioxidant molecules whose functions are the protection of sperm cells from oxidative damage. Among enzymatic scavengers, we have shown in earlier studies that the mammalian epididymis is the almost exclusive site of strong expression of one particular glutathione peroxidase (GPX), GPX5 (reviewed in ref. 4). This unconventional mammalian GPX, unlike the other members of the family, is devoid of the classical selenocysteine residue that was shown to be critical for its activity (5). *Gpx5* is strongly expressed under androgenic control in the caput epididymidis (6), and the corresponding protein is readily secreted in the epididymal lumen, where it was shown to interact loosely with sperm cells (7, 8). These expression characteristics were found to be quite conserved in all the mammals tested so far, including humans, suggesting that this enzyme might play a key role in the process of post-testicular sperm maturation. Other

**Conflict of interest:** The authors have declared that no conflict of interest exists.

**Nonstandard abbreviations used:** eSOD3, extracellular SOD3; GPX, glutathione peroxidase; mBrB, monobromobimane; MDA, malondialdehyde; 8-oxodG, 8-hydroxydeoxyguanosine; snGpx4, sperm-nucleus Gpx4 variant.

**Citation for this article:** *J. Clin. Invest.* **119**:2074–2085 (2009). doi:10.1172/JCI38940.

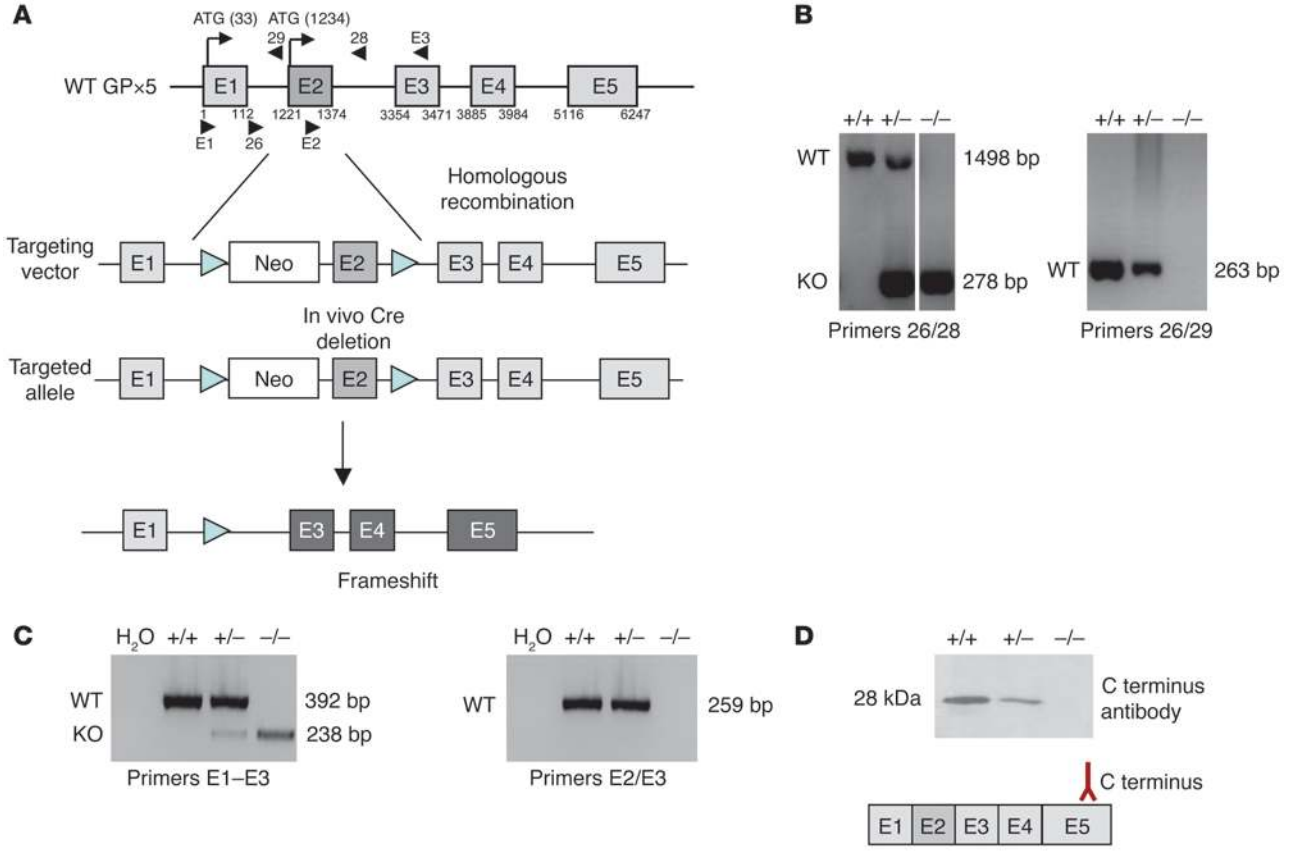


**Figure 1**

Generation of *Gpx5*-deficient mice. (**A**) Schematic representation of mouse *Gpx5* gene organization. Top: Gray boxes (E1 to E5) indicate the 5 GPX5 coding exons. Black arrows point to in-frame ATG translational start sites. Arrowheads indicate the relative positions of the various primers used in PCR amplification. Numbers (in bp) at the boundaries of each exon correspond to the GenBank *Gpx5* sequence (accession number NM_010343), with "1" indicating the cap site. Bottom: A scheme of the targeting vector and the resulting allele is shown. In vivo Cre-mediated excision of the *Gpx5* exon 2 led to a premature translation frameshift. (**B**) PCR experiments carried out on genomic DNA extracted from animal fingers. In the left panel, lanes were run on the same gel but were noncontiguous. (**C**) RT-PCR assays carried out with mRNA extracted from caput epididymal tissues. In **B** and **C**, the bp numbers indicate the size of the amplified products, and the primer pairs used are indicated at the bottom of each panel (see **A**). (**D**) Western blot assays carried out with caput epididymidis protein extracts and a polyclonal anti-GPX5 antibody directed against a C-ter synthetic peptide (31). The kDa number in the left margin indicates the size of the GPX5 full-length protein. +/+, +/–, and –/– indicate animals that were WT, KO heterozygous, or homozygous for GPX5. The $H_2O$ lanes correspond to a control amplification carried out on water.

selenium-containing GPXs (GPX1, GPX3, and GPX4) were found to be expressed by the mammalian epididymis but at much lower levels (9, 10). These epididymis-expressed GPXs differ from GPX5 in that they are cytosolic enzymes and therefore are not secreted in the epididymal lumen.

Besides their role as ROS scavengers (essentially recycling hydrogen peroxide, the product of SOD action), it has been shown that GPX enzymes can work as disulfide bridging intermediates (11, 12). This was exemplified recently by the role played by a testis-expressed and sperm-bound GPX, the sperm-nucleus GPX4 variant (snGPX4) that was shown in the presence of hydrogen peroxide to mediate disulfide bridges between thiol-containing protamines, thus increasing sperm DNA compaction during epididymal transit (13, 14). In recent years, it has became clearer that ROS (especially hydrogen peroxide) exert dual and opposite actions on sperm cells (2, 15). Basically, a certain level of ROS is necessary for disulfide bridging events that concern not only the sperm nucleus but also other protein-protein interactions on sperm plasma membrane, midpiece, and flagella (16–25). Hydrogen peroxide was also identified as a key signal transduction effector of tyrosine phosphorylation events that trigger sperm capacitation (26, 27) and ultimately acrosome reaction (reviewed in ref. 28). However, too much hydrogen peroxide results in cell-oxidative damages, eventually leading to cell death. These dual effects of ROS on sperm cell, both detrimental and beneficial, have led to the idea that a very fine tuning in the generation/recycling balance of hydrogen peroxide must exist in and around sperm cells (2, 15).

Because of the absence of the catalytic important selenocysteine residue in the GPX5 primary sequence, questions have arisen regarding the function of this protein in the mammalian epididymis. In earlier studies we showed that mouse GPX5 works, both in vitro and in vivo, as would be expected for a ROS scavenger (29, 30). In the present study, in order to determine the precise role of epididymal-secreted GPX5 protein in the post-testicular sperm maturation process, we report on the generation of a mouse *Gpx5* KO model. We describe the generation of the *Gpx5*-null mice and

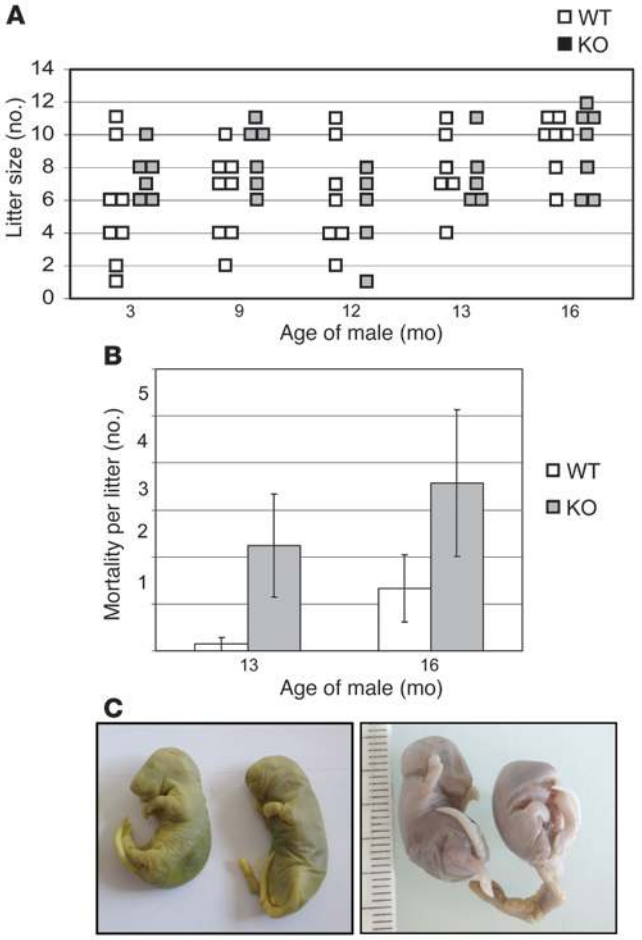


**Figure 2**
Impact of GPX5 deletion on mouse fertility. (**A**) Litter sizes (each gray or white square corresponds to an independent litter for *Gpx5* KO or WT males), with respect to the age of the males. Female mice had a WT genetic background. (**B**) Mortality of pups from matings between WT female mice and *Gpx5*$^{-/-}$ male mice aged 13 months and 16 months. Data are mean ± SEM. (**C**) Examples of aberrant development in 2 distinct cases of pregnancies reported in **B** (from matings with *Gpx5*$^{-/-}$ males aged 13 months).

subsequent experiments investigating the impact of the absence of GPX5 on male fertility. Overall, in the absence of GPX5, we did not record any drastic impact on the fertility potential of male mice. However, we noticed an increase in developmental defects when WT female mice were crossed with *Gpx5*$^{-/-}$ aging males (over 1 year old). A closer analysis of sperm cell integrity was conducted on these males using cytometry. Our analysis of the *Gpx5*$^{-/-}$ model was also completed by a detailed investigation of the expression of other epididymis-expressed GPXs as well as of other related ROS scavengers using quantitative RT-PCR. The latter analysis showed clearly that a regionalized antioxidant response was at stake in mouse cauda epididymidis of the *Gpx5*$^{-/-}$ animals, demonstrating a clear role for GPX5 in protecting sperm cells and cauda epididymidis tissue from ROS-mediated oxidative damages.

## Results

*GPX5 KO mouse generation and screening*. As shown in Figure 1, the *Gpx5* gene is made up of 5 exons spanning approximately 8 kb on mouse chromosome 13 (GenBank accession number NM_010343). Exon 1 encodes the secretion signal of the GPX5 protein. To disrupt the *Gpx5* gene, exon 2 was deleted through homologous recombination with the aim of generating a truncated transcript and a translation frameshift that would abolish the production of the GPX5 protein. A targeting vector containing the Neo cassette (for selection purposes) and exon 2 sequence, both flanked with LoxP sites, was generated (Figure 1A). ES cells from C57BL/6 mice were transformed by the targeting vector and screened via Southern blot for adequate recombination (data not shown). After injection of recombinant ES cells into blastocysts and reintroduction of the blastocysts into female mice prepared for gestation, chimera mice were created. Germ line transmission of the targeted allele was verified. First, matings between heterozygous *Gpx5* mice and *Cre*$^{+/+}$ mice were performed to generate mice free of the Neo cassette and exon 2. Then, intercrosses between *Gpx5*$^{+/-}$[Cre] mice were carried out to eliminate the Cre allele (a putative source of interferences with the mouse genome). When Southern blot analysis was performed on PCR-amplified DNA extracted from transgenic animals, we detected the presence of both WT and deleted alleles in heterozygous animals and no WT allele in homozygous *Gpx5*$^{-/-}$ animals, indicating that exon 2 deletion was effective (Figure 1B). Amplifications carried out on reverse-transcribed caput epididymidis RNA confirmed that the *Gpx5* exon 2 was deleted in the transgenic animals (Figure 1C). These results were in accordance with the genomic construct chosen for homologous recombination. In this strategy, *Gpx5* expression was maintained (i.e., there was generation of a truncated *Gpx5* mRNA in the epididymis of the KO animals), but the translated protein was limited to 30 amino acids (including part of the secretion signal) instead of 221 amino acids for the native GPX5 protein. To confirm that the truncated *Gpx5* mRNA detected in the *Gpx5*$^{-/-}$ animals would not lead to a noticeable detection of any GPX5 protein, Western blot analysis was carried out using a GPX5-polyclonal antiserum (31). Figure 1D shows that GPX5 protein expression was diminished in *Gpx5*$^{+/-}$ mice and abolished in *Gpx5*$^{-/-}$ mice. A survey of heterozygous *Gpx5* mouse crosses revealed that, among 101 pups generated, 51% were heterozygous, 31% were WT, and 18% were homozygous KO for GPX5. These proportions are compatible with a theoretical Mendelian distribution, suggesting that *Gpx5* is not essential for embryonic development and viability. Histological examination of epididymal tissues from the various parts of the organ (i.e., caput, corpus, and cauda) did not show any obvious macro- or microscopic differences between *Gpx5*$^{+/+}$ and *Gpx5*$^{-/-}$ animals. Tubule size and epididymis-constituting cell morphologies appeared equivalent to that observed in control animals (data not shown). Cauda sperm cell number, morphology, and velocity evaluated through the use of computer-assisted sperm analysis (Hamilton Thorne) and cytological Schoor staining were found to be similar to those of control animals at any age (see Supplemental Data; supplemental material available online with this article; doi:10.1172/JCI38940DS1).

*Evaluation of Gpx5*$^{-/-}$ *mouse fertility*. To investigate the effect of the absence of epididymal GPX5 expression on male fertility, male mice of the 2 genotypes (WT and *Gpx5*$^{-/-}$) were mated with WT C57BL/6 female mice. Matings were conducted using animals at optimal reproductive age (3 months). No changes in mating behavior were noticed. Three-month old male *Gpx5*$^{-/-}$ mice showed

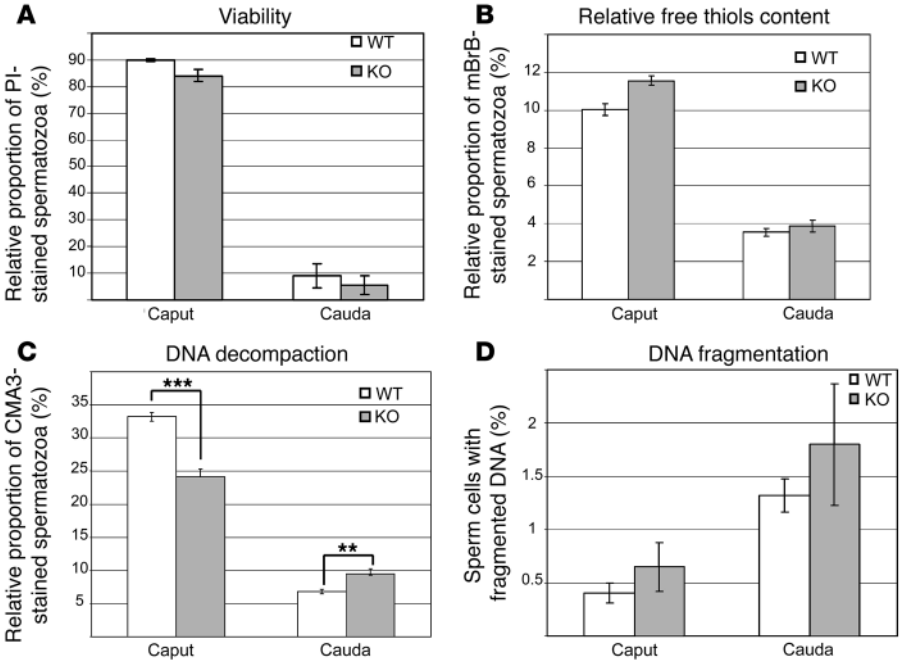


**Figure 3**
Evaluation of spermatozoa integrity by cytometry. (**A**) Evaluation of spermatozoa viability. Histograms show the incorporation of propidium iodide (PI) in spermatozoa from caput or cauda epididymides. (**B**) Disulfide bonds/free thiol quantification by mBrB staining. Histograms show the incorporation of mBrB. (**C**) Protamine association with sperm chromatin, as determined by chromomycin A3 (CMA3) staining. $^{**}P < 0.05$; $^{***}P < 0.01$. (**D**) Evaluation of sperm DNA fragmentation using the Halomax detection assay, based on the sperm chromatin dispersion test (55). Data are mean ± SEM. $n = 4$.

normal fertility, with litter size (7.3 ± 1.2 pups, $n = 6$) comparable to that of WT mice at the same age (5.9 ± 2.6 pups, $n = 8$) (Figure 2A). More matings were carried out using older male mice and WT female of proven fertility in order to determine whether the absence of GPX5 could have a greater effect upon aging. Figure 2A shows that, for 9- to 12-month-old animals, there were no statistically significant differences in litter sizes between *Gpx5*$^{-/-}$ (7.3 ± 2.7 pups, $n = 6$, and 5.6 ± 2.3 pups, $n = 5$, respectively) and WT backgrounds (6.6 ± 1.8 pups, $n = 8$, and 6.6 ± 2.2 pups, $n = 7$, respectively). Time to gestation in all these matings was monitored and was found to be comparable to that of WT crosses (data not shown). However, when using 1-year-old or older transgenic males, we started to record more miscarriages and developmental defects in our matings. This prompted us to have a closer look at pup mortality with aging males. As illustrated in Figure 2B, we observed an increase in the number of dead pups or aborted fetuses when matings were conducted with *Gpx5*$^{-/-}$ males aged 13 months and 16 months compared with control matings using WT animals at the same ages. This increased death toll was associated with various abnormal embryonic developments, examples of which are shown in Figure 2C (incomplete abdomen differentiation or eye differentiation for these 2 particular embryos recovered from the uterine horns of 2 distinct female mice). These developmental defects appeared heterogeneous, with no Mendelian inheritance (few pups in some litters, no viable pups in other litters) and with no links with pup genotypes, since all pups were heterozygous but not all were affected, at least macroscopically. One commonality shared by all the defective *Gpx5*$^{+/-}$ embryos we monitored was that the embryonic defects occurred at late developmental stages (i.e., during mid- or late organogenesis).

*Evaluation of Gpx5*$^{-/-}$ *sperm integrity*. As a first step toward understanding such apparently random and sporadic abnormalities in embryonic development we undertook a more thorough analysis of sperm cells from the *Gpx5*$^{-/-}$ transgenic animals. Since female mice used in the above-described matings were of a WT background, it was logical to assume that the developmental defects were *Gpx5*$^{-/-}$ male–linked. Spermatozoa viability assessment and functional membrane integrity appeared similar between WT and *Gpx5*$^{-/-}$ mice, according to flow cytometry measurements using propidium iodide as a probe (Figure 3A). The ability of spermatozoa to perform an acrosome reaction when challenged with hydrogen peroxide was also not modified (data not shown). Since the putative function of GPX5 is that of an antioxidant scavenger, we focused our attention on evaluation of oxidative injuries to sperm cells. Two parameters directly related to oxidative insults were investigated. First, using cytometry and monobromobimane (mBrB) as a probe, we determined the level of protein thiol redox status in sperm cells extracted from various epididymis parts by measuring the fluorescence of mBrB adducts. It is well established that during epididymal maturation, the number of spermatozoa-free thiols decrease considerably from caput to cauda (24), and this is exactly what we observed in our control WT animals and also in the transgenic animals (Figure 3B), although to a lesser extent. In both compartments (caput and cauda) there was no significant difference in the relative free thiol content when control animals were compared with *Gpx5*$^{-/-}$ animals, suggesting that GPX5 does not strongly participate in disulfide bridging events of thiol-containing sperm proteins during their epididymal descent. Second, we monitored the structural stability of sperm DNA. A rapid evaluation using exposure of caput or cauda sperm samples to 0.5% SDS did not display any significant nuclei decondensation when KO were compared with controls (data not shown). However, with a more refined approach using chromomycin A3 as a probe and cytometry to evaluate sperm DNA condensation, we did observe some differences. As expected (32, 33), spermatozoa DNA condensation was found to be higher in sperm cells from cauda epididymidis than in those from caput epididymidis (Figure 3C). This was also the case in *Gpx5*-null mice, although to a lesser extent. It is interesting to note that in caput sperm samples, sperm DNA compaction (which is negatively correlated with fluorescence intensity) was sig-

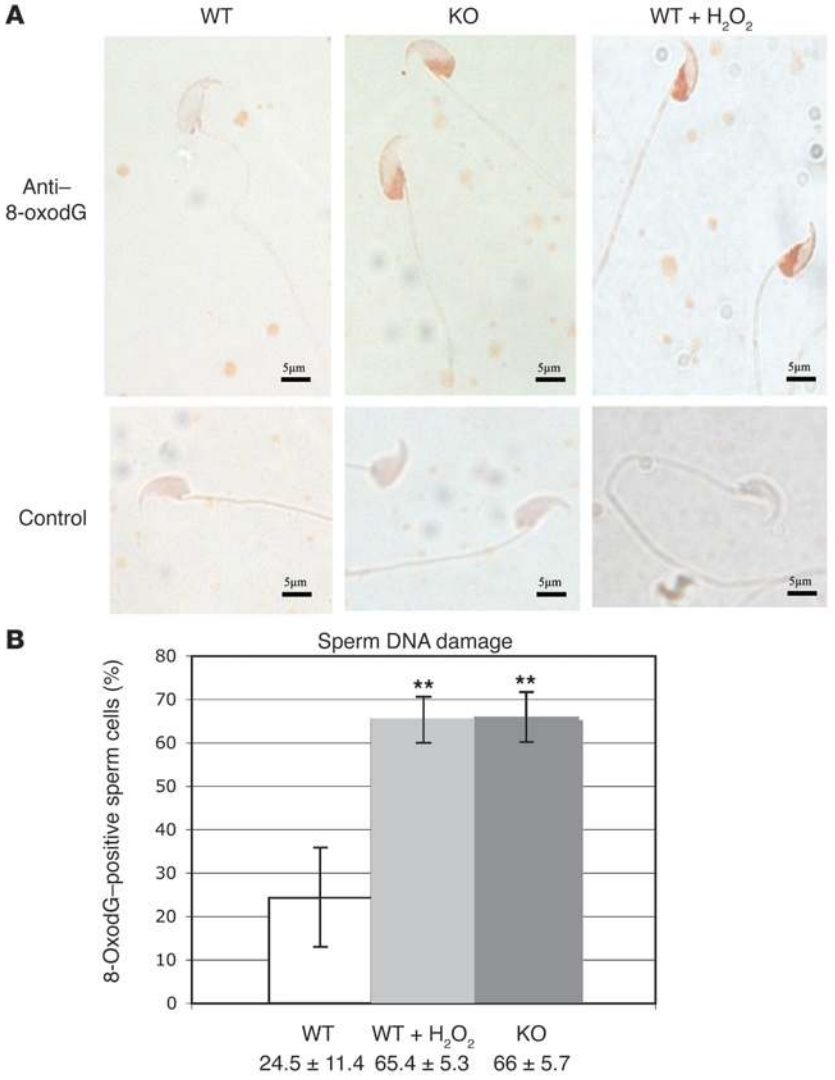


**Figure 4**

Cauda-retrieved spermatozoa of *Gpx5*$^{-/-}$ animals suffer oxidative damages. (**A**) Immunodetection of the nuclear adduct 8-oxodG in cauda epididymidis-retrieved spermatozoa preparations from 6-month-old WT, KO, or hydrogen peroxide–treated WT male mice. Images are representative of several distinct detections. (**B**) Histograms showing the percentage of 8-oxodG–positive spermatozoa in cauda epididymidis-retrieved spermatozoa preparations, from 6-month-old WT, KO, and positive control (WT spermatozoa treated with hydrogen peroxide) male mice. Data are mean ± SEM. $n = 3$. $^{**}P < 0.05$.

nificantly greater in *Gpx5*$^{-/-}$ animals when compared with controls, while there was less compaction in *Gpx5*$^{-/-}$ animals in cauda sperm samples (i.e., the *Gpx5*$^{-/-}$ cauda sperm samples appeared to have less condensed nuclei than the controls). These regionalized (caput versus cauda) changes in sperm DNA compaction for *Gpx5*$^{-/-}$ versus control samples are addressed in the Discussion.

Since sperm DNA compaction might depend on the level of DNA fragmentation (a well-known effect of ROS-mediated damage to DNA), we monitored the level of sperm DNA fragmentation in WT and *Gpx5*$^{-/-}$ genotypes using a commercially available kit (Halomax; Chromacell). In both genotypes (WT and *Gpx5*$^{-/-}$), DNA fragmentation was found to be higher in cauda versus caput sperm samples (Figure 3D). In agreement with the idea that there might be an increase in the oxidative insult of sperm DNA in *Gpx5*$^{-/-}$ animals, the fragmentation of sperm DNA was found to be at its highest in *Gpx5*$^{-/-}$ cauda samples. The difference was not found to be statistically significant in *Gpx5*$^{-/-}$ sperm samples due to large variations among individuals. However, it is worth noting that all control samples were found to be homogenous (small standard errors), while the transgenic samples presented a large interindividual variability (large standard errors), reflecting the interindividual variations recorded in the occurrence of developmental defects when aging *Gpx5*$^{-/-}$ animals were mated with WT females (see above). Since the sensitivity of the Halomax detection system does not allow for the detection of low levels of DNA fragmentation, we monitored the apparition of 8-hydroxy-deoxyguanosine (8-oxodG) on sperm DNA through the use of an 8-oxodG antibody that specifically recognizes DNA damages created by oxidative attacks on DNA. Typical results of 8-oxodG detection, presented in Figure 4A, indicate that cauda-retrieved spermatozoa from *Gpx5*$^{-/-}$ animals were highly reactive toward the 8-oxodG monoclonal antibody, while WT controls were not. A positive control, in which WT spermatozoa prior to the detection were treated with hydrogen peroxide to induce oxidative damages, showed a response very similar to that of the *Gpx5*$^{-/-}$ animals. The data presented in Figure 4B illustrate the numbers of 8-oxodG–positive cells counted on 3 distinct pools of cauda-retrieved spermatozoa from WT and *Gpx5*$^{-/-}$ animals aged 6 months. Hydrogen peroxide–treated, WT cauda-retrieved spermatozoa samples were used as positive controls. As illustrated in Figure 4B, the quantity of 8-oxodG was found to be significantly increased in *Gpx5*$^{-/-}$ sperm samples at a level quite comparable to hydrogen peroxide–treated WT sperm samples.

*A lack of epididymis-luminal GPX5 in Gpx5*$^{-/-}$ *animals leads to oxidative stress*. The observation that *Gpx5*$^{-/-}$ cauda-stored sperm DNA suffered from ROS-mediated damages prompted us to investigate whether or not an oxidative stress was at stake in the epididymides of *Gpx5*$^{-/-}$ animals. To do so, expression levels of GPX1, GPX3, and GPX4, the 3 classical cytosolic GPXs in the epididymis that, together with GPX5, were found to be expressed in the mouse epididymis, were investigated using quantitative RT-PCR (Figure 5, A and B). In agreement with earlier studies, among these 3 cytosolic GPXs, GPX3 was found to be the most strongly expressed in the mouse epididymis, while GPX4 and GPX1 were expressed at lower levels. In agreement with previous data, cauda expression of GPX3 and, to a lesser extent, that of GPX4, were stronger than caput expression. Comparison of transgenic and WT animals (6 months old) showed that while the accumulation of the 3 cytosolic *Gpx* mRNAs was not changed in the caput compartment, it was significantly increased in the cauda compartment of the *Gpx5*-null mice (Figure 5, A and B). In parallel, total GPX activity was assayed in caput and cauda

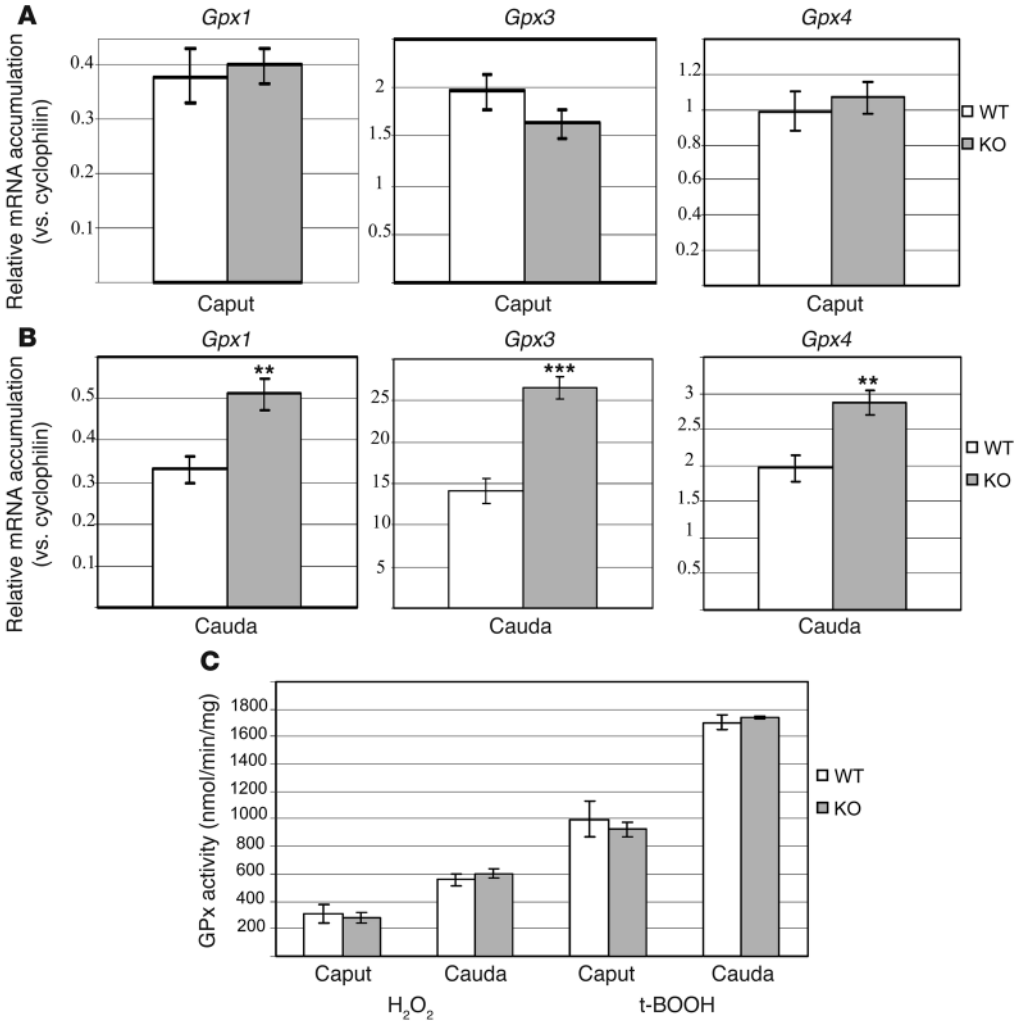


**Figure 5**
GPX5 deficiency leads to cauda epididymidis oxidative response. (**A** and **B**) Quantitative RT-PCR estimations of *Gpx1*, *Gpx3*, and *Gpx4* mRNA accumulations in caput (**A**) and cauda (**B**) epididymidis samples from WT and KO male mice. Data are mean ± SEM. $n = 2$. (**C**) Analysis of global GPX activity using either hydrogen peroxide or *tert*-butyl hydroperoxide (t-BOOH) as a substrate. Data are mean ± SEM. $^{**}P < 0.05$; $^{***}P < 0.01$.

protein extracts in the 2 genetic backgrounds using 2 different but classical substrates for GPX activity: a physiological substrate (hydrogen peroxide) and a non-physiological but conventional substrate (*tert*-butyl hydroperoxide). In agreement with previous data, total GPX activity was found to be twice as strong in cauda compared with caput. As shown in Figure 5C, we recorded no difference in total GPX activity when caput and cauda samples from 6-month-old *Gpx5*$^{-/-}$ animals were compared with controls.

To complete this study of epididymis enzymatic scavengers status, we also monitored, using quantitative RT-PCR, accumulations of other members of the redox catalytic triad (i.e., SOD, catalase, and GPX; see Figure 6A). Figure 6B shows the expression levels of catalase and extracellular SOD3 (eSOD3; known to be expressed in the mouse cauda epididymidis). It appeared that accumulation of eSOD3 was not different either in caput or cauda epididymides compartments when *Gpx5*$^{-/-}$ animals were compared with WT animals. Interestingly, the relative accumulation of catalase mRNA in cauda epididymidis samples from *Gpx5*$^{-/-}$ animals was found to be significantly increased compared with controls, while it was not changed in the caput territory.

*Cauda epididymidis epithelia and spermatozoa of Gpx5*$^{-/-}$ *animals suffer from peroxidative injuries*. The increased expression of epididymis cytosolic GPXs (GPX1, GPX3, and GPX4) and of cytosolic catalase in cauda epididymidis samples from *Gpx5*$^{-/-}$ animals suggested that the cauda territory of transgenic animals was subjected to ROS-mediated oxidation. In agreement with this hypothesis, Figure 7A shows histologic sections of cauda epididymidis tissues from *Gpx5*$^{-/-}$ animals, in which a clear and strong labeling of cauda epithelial cell nuclei was evident when using the 8-oxodG antibody, a classical marker of cell DNA oxidative injury. Such strong nuclear labelling was not seen in WT cauda epididymidis sections. This attests that the *Gpx5*$^{-/-}$ cauda tissue indeed suffers from oxidative damage. In parallel, we also monitored the levels of malondihaldehyde (MDA) compound, a final product of lipid peroxidation in cauda-retrieved sperm samples from WT and *Gpx5*$^{-/-}$ animals. Data, presented in Figure 7B, confirmed that cauda spermatozoa from *Gpx5*$^{-/-}$ animals suffered from lipid peroxidation, since MDA accumulation was twice that of control samples.

## Discussion

The *Gpx5* gene has long been reported to be a highly tissue-restricted gene expressed, in all the mammals that have been tested so far, under androgenic control only within the adult epididymis (8). In several mammals, the corresponding GPX5 protein is one of the major secretory products of the caput epididymidis. Based on sequence identity, GPX5 belongs to the *Gpx* enzymatic gene family

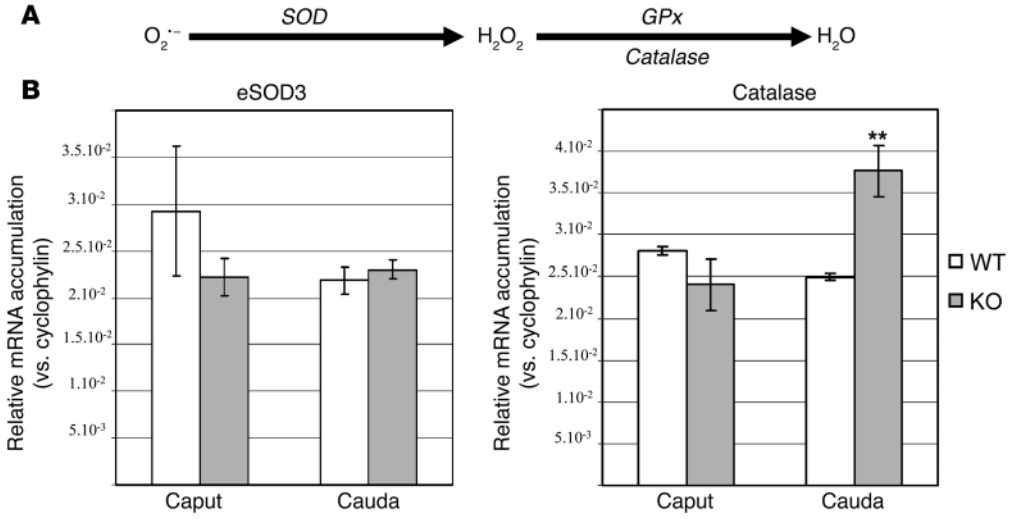


**Figure 6**
Catalase, but not eSOD3, participates in the antioxidant response of the *Gpx5*$^{-/-}$ cauda epdidymidis. (**A**) Schematic representation of the ROS recycling pathway using the catalytic triad of scavengers. (**B**) Quantitative RT-PCR estimations of eSOD3 and catalase mRNA accumulations in caput and cauda epididymis samples from WT and KO male mice, using the cyclophilin transcript as a reference. Data are mean ± SEM. $n = 2$. $^{**}P < 0.05$.

that encodes proteins recycling hydrogen peroxide and also more complex peroxidized substrates (6, 8). Within the mammalian GPX protein family, GPX5 is a unique enzyme, since it is devoid of the classical selenocysteine residue that is part of the GPX catalytic site and that was shown to be critical for selenium-dependent GPX activity (5). Despite the absence of this essential residue in its catalytic site, we have shown in earlier studies that GPX5 could work both in vitro and in vivo, as would be expected for an antioxidant scavenger (29, 30). The conservation of GPX5 among mammalian species as well as its strict tissue restriction has led researchers to propose that this protein could fulfill an important function in the post-testicular process of epididymal sperm maturation. The generation of a *Gpx5*-null mouse model was therefore undertaken to determine more precisely the function of GPX5 in mammalian epididymis physiology. We describe here the production of the *Gpx5* KO mouse model. The loss of accumulation of the GPX5 protein in the epididymis of transgenic animals was ascertained by Western blotting assays. In accordance with the tissue-restricted and late postnatal male-specific expression of the *Gpx5* gene, *Gpx5* extinction did not affect animal viability. To date, other GPX KO mouse models have been generated, including *Gpx1* (also called *Cgpx*), *Gpx4* (also called *Phgpx*), and *Sngpx4* (also called *Snphgpx*) (13, 34, 35). Only the extinction of *Gpx4* was shown to affect mouse viability and was accompanied by early developmental defects (35, 36). A light microscopic analysis of the epididymis tissues of *Gpx5*$^{-/-}$ animals did not reveal any disturbance in its organization or cytology. Also, the number and cytology of sperm cells were found to be identical (at least at a macroscopic level) to that of control animals, whatever their age. Regarding the fertility of the *Gpx5*$^{-/-}$ males, our investigations have shown that the lack of GPX5 expression had no drastic impact on their fertility score (as evaluated by litter size and delay in conception) when the transgenic males were young. With aging transgenic males (over 1 year old), we started to notice a decrease in the number of viable pups when compared with control matings using WT animals of the same age. Miscarriages and a large array of late developmental defects were monitored with aging *Gpx5*$^{-/-}$ males. Since GPX5 is restricted only to the male genital tract and the female mice we used in our matings were of the WT genotype, we inferred that the miscarriages and developmental defects observed with *Gpx5*$^{-/-}$ aging males resulted from the quality of the spermatozoa themselves. It is well documented that any damage to the sperm DNA integrity has an impact on reproductive capacity (reviewed in ref. 37). In humans, clinical evidence has clearly shown that sperm DNA damage may adversely affect reproductive outcome and that the spermatozoa of infertile men possess more DNA damage than the spermatozoa of fertile men (38–43). The fact that we observed only late developmental defects in embryos obtained with aged *Gpx5*$^{-/-}$ males is also in agreement with the conclusion reached by Tesarik et al. (44, 45), who found that late, but not early, paternal effects on human embryo development were related to sperm DNA damage.

Among etiologic factors that are suggested to explain sperm DNA damage, ROS-mediated attacks of sperm DNA occupy a central position. During epididymal transit of sperm cells, there are 2 main ways by which ROS can alter sperm DNA integrity. First, ROS can interfere with post-testicular chromatin packaging. During epididymal transport thiol-containing protamines, and consequently sperm DNA, are increasingly compressed through intermolecular and intramolecular disulfide cross-linking (23, 43, 46). Interestingly, a sperm nucleus–specific isoform of GPX4, snGPX4, was proposed to be involved in such disulfide bridging events in the presence of hydrogen peroxide (12). This was recently confirmed by the generation of the *Sngpx4*$^{-/-}$ mouse model, in which the authors noticed that the absence of *Sngpx4* expression leads to a delay in epididymal sperm DNA compaction (13). In this transgenic model, final sperm DNA compaction was not significantly altered, but it occurred later during sperm epididymis transit (i.e., in the cauda epididymidis rather than in the caput, as is the case in WT animals), suggesting that other enzymes could compensate in the absence of snGPX4 (13). Although the authors proposed that the cytosolic form of GPX4 could be responsible for this compensatory effect, we hypothesized that this could also come from the secreted and sperm-bound GPX5 protein (8). The data reported here using mBrB as a probe and cytometry proved that we were wrong, since the data show that the absence of *Gpx5* expression in the transgenic animals produced no change at all in the ratio of free thiols to disulfides when compared with control animals, regardless of the territory of the epididymis (caput or cauda). This rules out the possibility that GPX5 could participate in overall disulfide bridging events of sperm proteins and,

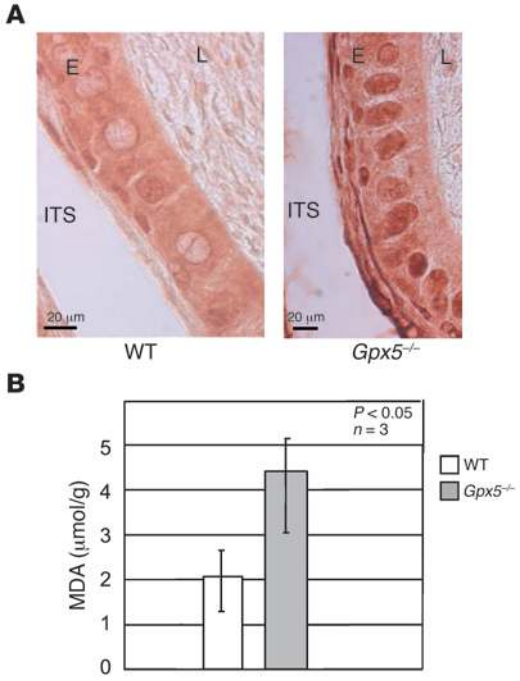


**Figure 7**
The cauda epididymidis epithelium of *Gpx5*$^{-/-}$ animals suffers from oxidative damage. (**A**) Detection of the nuclear 8-oxodG modification in cauda epididymidis epithelium sections of 14-month-old WT and *Gpx5*$^{-/-}$ male mice. Note the strong and uniform nuclear labeling in the *Gpx5*$^{-/-}$ section. L, lumen; E, epithelium; ITS, intertubular space. (**B**) MDA measurements on cauda-collected spermatozoa samples from 6-month-old WT and *Gpx5*$^{-/-}$ animals. Data are mean ± SEM.

consequently, in the control of sperm DNA packaging via disulfide bridging. The second argument against GPX5 involvement in disulfide bridging of sperm DNA protamines came from our observation that the *Gpx5*$^{-/-}$ caput sperm DNA compaction was significantly greater than that of the control animals. If GPX5 was involved in protamine disulfide bridging events, one would have expected the opposite effect (i.e., less condensation of the caput sperm nuclei in *Gpx5*$^{-/-}$ animals). The increased caput sperm DNA compaction of *Gpx5*$^{-/-}$ animals we observed could well be explained by the fact that, GPX5 being absent from the caput lumen, there is more hydrogen peroxide (or other ROS) available for snGPX4-mediated or direct disulfide bridging action of thiol residues on protamines, thus allowing a greater compaction of caput sperm DNA. This is in agreement with the observations made by Conrad et al. (13), who clearly showed that snGPX4 exerts its action on sperm protamine disulfide bridging in the caput epididymidis territory.

The second way in which ROS may alter sperm DNA integrity is by direct oxidation of DNA or, through caspase-mediated apoptotic actions, by creating single-strand or double-strand breaks (47, 48). This may result in sperm DNA fragmentation, which has been positively correlated with fertilization performances of aging males or/and infertile men as well as in reproductive outcomes after in vitro fertilization (37, 40). The major sources of ROS in the male reproductive tract were reported to be due to leukocyte infiltrations following inflammatory or infectious conditions (49). However, in non-infectious situations, there are other sources of ROS and spermatozoa themselves are considered to be good ROS producers. One way in which epididymal sperm could produce ROS is through leakage of electrons from the mitochondrial chain transport (50). This hypothesis was recently supported by the observation that the spermatozoa of mice lacking transaldolase (an enzyme of the non-oxidative phase of the pentose phosphate pathway) exhibit defective mitochondria lacking membrane potential and showing reduced levels of NADH and GSH as well as impaired ROS generation (37). More recently, the work of Koppers et al. (51) suggested mitochondria-generated ROS as good candidates for oxidative stress in human spermatozoa. This sperm ability to produce ROS is a risky situation, particularly for cauda-stored spermatozoa that are fully functionally mature (i.e., ready to express their motility), having completed the epididymis maturation processes. In accordance with the idea that cauda-stored sperm are at risk of oxidative stress is the presence in the cauda epididymidis luminal fluid of a SOD enzyme (eSOD3) and the strong accumulation of the GPX5 (8). The eSOD3 is there to recycle superoxide anions consequently generating hydrogen peroxide that, in turn, will be transformed into water by the luminal GPX5. Also in agreement with a physiological oxidative stress situation in the cauda epididymidis luminal compartment is our earlier observation that the cauda epithelium protects itself from hydrogen peroxide–mediated damages (hydrogen peroxide can diffuse from one cell to another, while superoxide anion cannot) by the strong cytosolic expression of GPX3 (the plasma-type GPX) within the cauda epithelium, while GPX3 expression is weaker in the corpus and the caput compartments (10). The observations we have made in the cauda epididymides of the *Gpx5*$^{-/-}$ animals are in line with this situation. First, it was found that cauda epithelium of *Gpx5*$^{-/-}$ animals was engaged in an oxidative stress response. This was supported by the fact that the 3 epididymal cytosolic GPXs (GPX1, GPX3, and GPX4) were transcriptionally upregulated only in the cauda compartment of *Gpx5*$^{-/-}$ animals, suggesting that these animals had to cope with elevated levels of ROS within the cauda territory. In addition, we observed that catalase mRNA accumulation was also increased in the cauda epididymides of *Gpx5*$^{-/-}$ animals, reinforcing the idea that the tissue has to face oxidative stress, presumably because of elevated hydrogen peroxide levels. The fact that the relative mRNA accumulation of the cauda luminal eSOD3 was not changed in the cauda epididymidis *Gpx5*$^{-/-}$ samples suggests either that there was no change in the production of superoxide anion or that the enzyme activity was not limiting. In any case, the absence of GPX5 in the lumen of KO animals led to a transcriptional antioxidant response within the cauda epididymidis epithelium, as indicated by the increased mRNA accumulation of cytosolic GPXs and catalase. The absence of significant change in total GPX activity when GPX5 was absent suggests that the cauda epididymidis of transgenic animals (at 6 months of age) somehow compensates for the GPX5 deficiency. Since it is well established that the activities of sperm antioxidant scavengers gradually decrease with age (52), it is likely that *Gpx5*$^{-/-}$ animals increasingly suffer from oxidative stress when aging.

The suspicion of cauda oxidative stress in *Gpx5*$^{-/-}$ animals is further supported by the fact that there was a greater reactivity of the *Gpx5*$^{-/-}$ cauda epididymidis epithelium (when compared with control cauda sections) toward the 8-oxodG antibody, a

**Table 1**
Oligonucleotide primers used in quantitative PCR assays

| Target gene | 5′–3′ primer sequences | Product length (bp) | Melting temperature (°C) |
|---|---|---|---|
| *Gpx5* | 26 F, GTGTCTGAGAATCTAGTCCTAGC | 1,498 | 60 |
| | 28 R, GTGACAGTTTTCTCAGGGGTTGG | | |
| | 26 F, GTGTCTGAGAATCTAGTCCTAGC | 263 | 60 |
| | 29 R, CTGCCTTGTGAAGGTTGACAGG | | |
| | E1 F, AGGCCCTCAGACCAGAAATC | 392 | 58 |
| | E3 R, TTGAGCCCAGGAAGAATCTC | | |
| | E2 F, AAGACGTGAAAGGCACCATC | 259 | 58 |
| | E3 R, TTGAGCCCAGGAAGAATCTC | | |
| *Gpx1* | F, GTCCACCGTGTATGCCTTCT | 217 | 62 |
| | R, CTCCTGGTGTCCGAACTGAT | | |
| *Gpx3* | F, GATGTGAACGGGGAGAAAGA | 173 | 62 |
| | R, TTCAAGCAGGCAGATACGTG | | |
| *Gpx4* | F, AGTACAGGGGTTTCGTGTGC | 410 | 62 |
| | R, CGGCAGGTCCTCTATCA | | |
| Catalase | F, GCAGATACCTGTGAACTGTC | 229 | 60 |
| | R, GTAGAATGTCCGCACCTGAG | | |
| eSOD3 | F, GCTCTCAGAGAACCCCTCT | 170 | 60 |
| | R, GTGCTATGGGGACAGGAAGA | | |
| Cyclo A | F, GGAGATGGCACAGGAGGAA | 76 | 60 |
| | R, GCCCGTAGTGCTTCAGCTT | | |

Cyclo A, cyclophilin A.

classical nuclear marker of DNA oxidative injury. Regarding spermatozoa themselves, our data show that condensation of cauda sperm nuclei from aged (over 15 months old) *Gpx5*$^{-/-}$ animals was significantly lower than that of control animals at the same age, suggesting that the integrity of the *Gpx5*$^{-/-}$ cauda sperm cell DNA was altered. This observation is correlated with the data showing that the *Gpx5*$^{-/-}$ cauda sperm DNA is highly reactive toward the 8-oxodG monoclonal antibody, revealing oxidative attacks of the sperm DNA. This is also in agreement with our observation that the fragmentation level of the aged *Gpx5*$^{-/-}$ cauda sperm DNA tended to be greater (as revealed by the use of the Halomax kit) than that of the cauda sperm samples from control animals at the same age. Increased cauda sperm fragmentation is what one would expect from cauda-localized oxidative stress. Reinforcing the idea that cauda-stored spermatozoa of *Gpx5*$^{-/-}$ males are subjected to oxidative damage is our observation of the increased accumulation of the lipid peroxidized adduct, MDA.

Altogether, the data we have collected strongly suggest that the cauda epididymides of *Gpx5*$^{-/-}$ animals, and consequently the male gametes stored in it, were under oxidative stress. Our interpretation of the situation is that the lack of luminal GPX5 activity does not allow for a proper luminal ROS recycling, a state that seems to be exacerbated in aging animals, in agreement with the well-known free radical theory of aging. This theory sustains that, upon aging, the improper recycling of free radicals, resulting from a decrease in antioxidant protection (i.e., decrease in enzymatic activity of the various antioxidant scavengers), renders cells more susceptible to oxidative insults (reviewed in ref. 53). Our work suggests GPX5 as an important epididymal luminal scavenger, at least in the mouse, helping to protect both sperm cell DNA integrity and the cauda epididymidis epithelium from ROS-mediated oxidative insults. Our data also suggest that the storage of sperm in the cauda epididymidis, again at least in the mouse, is a challenging situation in terms of the exposure of the sperm to oxidative stress. It indirectly supports the idea that, while stored in the cauda epididymidis compartment, the spermatozoa themselves are likely to be responsible for the production of the harmful ROS. To our knowledge this is the first report showing that an imbalanced post-testicular epididymal luminal redox environment is detrimental to embryo viability. These findings are particularly relevant to male fertility in humans (reviewed in ref. 54). They support the clinical observations that have linked age-related DNA damage to human spermatozoa with a range of adverse clinical outcomes including depressed fertility, an increase incidence of miscarriage, and morbidity in the offspring, including childhood cancer.

## Methods

### *Generation of Gpx5 KO mice*

*Vector construction*. Mouse genomic fragments for the long arm, short arm, and floxed arm were subcloned from a genomic C57BL/6 RP23 BAC library and recloned into the basic targeting vector harbouring loxP sites, an FRT flanked Neo cassette for positive selection, and a ZsGreen cassette for counter selection (Figure 1). The confirmed sequence of the final targeting vector is available in the Supplemental Data.

*ES cell culture*. The C57BL/6N ES cell line was grown on a mitotically inactivated feeder layer comprised of mouse embryonic fibroblasts in DMEM high-glucose medium containing 20% FBS (PAN) and 1200 U/ml leukemia inhibitory factor (Millipore; catalog ESG 1107). Cells ($10^7$) and 30 ng of linearized DNA vector were electroporated (using the BioRad Gene Pulser) at 240 volts and 500 microfarads. G418 selection (200 μg/ml) started on day 2 after electroporation. ES clones were isolated on day 8 and screened by Southern blotting according to standard procedures. After expansion and freezing in liquid nitrogen, external and internal probes were used to validate clones.

*Generation of mice*. KO mice were produced in the animal facility at TaconicArtemis GmbH in microisolator cages (Tecniplast Sealsave). After administration of hormones, superovulated Balb/c Ola/Hsd females were mated with Balb/c Ola/Hsd males. Blastocysts were isolated from the uterus at 3.5 dpc. For microinjection, blastocysts were placed in a drop of DMEM with 15% FCS under mineral oil. A flat tip, piezo-actuated microinjection pipette with an internal diameter of 12–15 μm was used to inject 10–15 targeted C57BL/6 N.tac ES cells into each blastocyst. After recovery, 8 injected blastocysts were transferred to each uterine horn of 2.5-dpc pseudopregnant NMRI females. Chimerism was determined according to coat color (black/white, indicating the contribution of ES cells to the Balb/c host). One homologously recombined clone harboring the targeted allele was used for the generation of chimeric mice by blastocyst injection. Highly chimeric mice were bred to C57BL/6 females, and offspring heterozygous

for the targeted allele were identified by Southern blot. To eliminate the selection marker and exon 2, mice heterozygous for the targeted allele were bred with mice carrying 1 copy of the Cre recombinase transgene under the control of the ROSA26 locus (C57BL/6-Gt[ROSA]26Sortm16[Cre]Arte). The resulting offspring, heterozygous for the null allele (C57BL/6-*Gpx5tm1115_.2 Arte*), was backcrossed with C57BL/6 mice to eliminate the Cre recombinase transgene. WT and mutant animals were derived from heterozygous intercrosses and were devoid of the Cre recombinase transgene. Mice were maintained on a 14-hour light/10-hour dark cycle and provided with food and water ad libitum. All animal procedures were run according to German animal welfare laws and with the permission of the District Government of Berlin. Once housed in the French animal facility, mice were maintained in conditions of controlled temperature (22°C) and a 12-hour light/12-hour dark cycle with food and water ad libitum. All animal procedures were run according to the French guidelines on the use of living animals in scientific investigations with the approval of the Comité Régional d'Ethique en Expérimentation Animale d'Auvergne.

*Genotyping of mice by PCR*. Genomic DNA was extracted from 1- to 2-mm-long tail tips using the NucleoSpin Tissue kit (Macherey-Nagel). Genomic DNA (2 μl) was analyzed by PCR in a final volume of 50 μl in the presence of 2.0 mM $MgCl_2$, 200 μM dNTPs, 100 nM of each primer, and 2.5 U of Taq DNA polymerase (Invitrogen) by running 2 independent PCR reactions. PCR1 with primer pairs 26 and 28 (Table 1) detected the presence of the conventional allele (1,498 bp), while PCR2 with primer pairs 26 and 29 (Table 1) detected the presence of the WT allele (263 bp). Following a denaturing step at 95°C for 5 minutes, 35 cycles of PCR were performed, each consisting of a denaturing step at 95°C for 30 seconds, followed by an annealing phase at 60°C for 30 seconds and an elongation step at 72°C for 1 minute. PCR was finished by a 10-minute extension step at 72°C. Amplified products were analyzed on a 2% agarose gel.

### *GPX5 expression assays*

*RT-PCR*. Total RNA was isolated from epididymis using Trizol Reagent (Invitrogen) according to the manufacturer's instructions. The concentration of total RNA was measured by absorbance at 260 nm, and purity was estimated by the 260/280-nm ratio. First-strand cDNAs were synthesized with reverse transcriptase and oligo-dT (Promega) according to the manufacturer's recommendations. Aliquots of cDNA (2 μl) were amplified using Taq DNA polymerase (Bioline, Abcys) with the primer pairs indicated in Figure 1 and Table 1, under the conditions described above.

*Western blot*. GPX5 protein expression in epididymis from KO and WT mice was determined by Western blot. Tissues were homogenized in a buffer consisting of 50 mM Tris-HCl, pH 7.6, 0.1 mM EDTA. The homogenates were centrifuged at 10,000 *g* for 10 minutes at 4°C to eliminate unbroken cells. Protein concentration was assayed using a kit based on the Bradford assay (BioRad). Each protein sample (20 μg) was subjected to reducing conditions, separated on a 12% SDS-PAGE, and transferred onto nitrocellulose membrane (Hybond-ECL; Amersham Biosciences). Blots were blocked for 1 hour with 10% (wt/vol) skim milk in PBS and incubated overnight with 2 anti-GPX5 rabbit polyclonal antibodies. GPX5 antibodies were directed against synthetic peptides localized either in the N terminus or the C terminus extremity of GPX5. Membranes were washed, incubated with a peroxidase-conjugated anti-rabbit IgG secondary antibody (dilution 1:10,000; Sigma-Aldrich), and revealed using the ECL detection system (Amersham Biosciences) according to the manufacturer's instructions.

### *Sperm preparation*

Sexually mature male C57BL/6 mice were killed by $CO_2$ inhalation. Epididymides were removed and freed of connective tissues and fat. Epididymides were further divided into caput, corpus, and cauda territories. Tissues were transferred in a small glass dish containing 1 ml of M2 medium (Sigma-Aldrich). To recover sperm cells, repeated punctures with a 26-gauge needle were performed to the caput or cauda tissues. After 5 minutes of incubation to allow for sperm cell dispersion, sperm suspensions were centrifuged (500 *g* for 5 minutes) and pellets were resuspended into 200 μl of M2. Sperm counts were determined using a Malassez hemocytometer apparatus. Cauda epididymides were removed and minced in Whitten's HEPES medium (20 mM HEPES, pH 7.3, 100 mM NaCl, 4.7 mM KCl, 1.2 mM $KH_2PO_4$, 1.2 mM $MgSO_4$, 5.5 mM glucose, 1 mM picric acid, 4.8 mM lactic acid) on ice, and sperm were collected as described above. Computer-assisted sperm analysis parameters were determined immediately after collection. Sperm tracks (300 frames) were captured using a CEROS sperm analysis system (Hamilton Thorne; software version 12).

### *Cytometry*

Spermatozoa of caput or cauda epididymides were diluted with M2 medium down to $10^6$ sperm cells/ml. Flow cytometer evaluation was performed using a Calibur cytometer (Becton Dickinson). For each analysis, 10,000 events were counted using specific probes as described above. Argon laser excitation at 488 nm was coupled with emission measurements at 530/30 band pass (red), 585/42 band pass (green). Nonspecific sperm events were gated out. The data were analyzed with Becton Dickinson CellQuest Pro Logiciel. Percentages of living and dead cells were assessed using propidium iodide (0.01 mg/ml; Sigma-Aldrich). Propidium iodide was incubated with sperm cells for 8 minutes at 37°C, then cells were analyzed by cytometry on the FL3 channel (>650 nm). Sperm total thiol contents were determined using mBrB as a probe (Thiolyte; Calbiochem). A 50-mM solution stock was diluted in 100% acetonitrile. Sperm cells were stained with 1 mM mBrB for 30 minutes at 25°C, then washed twice with PBS. Free thiols were measured by fluorescence on FL1 channel (515–545 nm). To evaluate sperm chromatin condensation, sperm cells were stained with 0.25 mg/ml chromomycin A3 (CMA3; Sigma-Aldrich) for 20 minutes at 25°C. Sperm nuclei decondensation levels were measured with a cytometer on the FL2 channel (564–606 nm). Assessment of sperm DNA fragmentation was carried out using the staining protocol of the Halomax kit (Chromacell).

### *Quantitative RT-PCR*

Real-time PCR assays were performed on an iCycler apparatus (BioRad). A cDNA template (2 μl; 1:50 dilution) was amplified by 0.5 U of HotMaster TaqDNA polymerase (BioRad) using SYBR Green dye to measure duplex DNA formation, following the manufacturer's instructions. Sequences of primer pairs used during the course of the study are provided in Table 1.

### *GPX assay*

Analyses of GPX activity were performed as previously described (29) using *tert*-butyl hydroperoxide (200 μM) and hydrogen peroxide (100 μM) as substrates. NADPH oxidation was monitored at 340 nm.

### *Evaluation of peroxidative damages*

8-oxodG detection was performed on cauda epididymidis tissue sections and spermatozoa. Cauda spermatozoa were collected as described above for cytometric analyses. Subsequently, spermatozoa were resuspended in a decondensing buffer consisting of 2 mM DTT and 0.5% triton X-100 in PBS 1× and incubated for 30 minutes at room temperature. After centrifugation at 500 *g* for 5 minutes at room temperature, spermatozoa were resuspended in 1 ml PBS, numbered, and deposited onto a glass plate (30,000 cells/plate). Cauda epididymidis paraffin-embedded tissue sections were prepared as described earlier (8). WT and *Gpx5*$^{-/-}$ spermatozoa or tissue sections were then compared for their reactivity toward the

8-oxodG monoclonal antibody (N45.1; Gentaur, Euromedex) (1:10 dilution in a saturating buffer provided with the antibody). As a positive control of oxidative damage of sperm DNA, a WT spermatozoa aliquot fraction was treated for 2 hours at room temperature by 5 mM hydrogen peroxide. Incubations with the primary antibody were conducted overnight at 4°C. Then, after 2 washes in PBS 1× (5 minutes each), the secondary antibody was applied for 30 minutes at room temperature (1:1,000 dilution). The detection was conducted with the use of the Vectastain ABC kit rabbit peroxidase IgG (Vector Laboratories). Signal amplification was obtained by the use of the Vector Nova Red substrate kit for peroxidase (Vector Laboratories). Lipid peroxidation in the tissues was measured by the thiobarbituric acid–reacting substance and was expressed in terms of MDA content. Sample aliquots were incubated with 10% trichloroacetic acid and 0.67% thiobarbituric acid. The mixture was heated on a boiling water bath for 30 minutes, an equal volume of N-butanol was added, and the final mixture was centrifuged. The organic phase was collected for fluorescence measurements. Samples assayed for MDA contained 1 mM butylated hydroxytoluene in order to prevent artifactual lipid peroxidation during the boiling step. The absorbance of samples was determined at 532 nm. Results were expressed as μmol MDA g–1 protein.

### *Statistics*

A 2-tailed Student's *t* test was performed to determine significant differences between groups, with a *P* value of less than 0.05.


## Acknowledgments

This work was supported by grants from the CNRS, INSERM, the French Ministry of Education and Research and a Grant in aid (SCH093) to J.R. Drevet and P. Vernet from the Ernst Schering Research Foundation, the Rockefeller Foundation, and the CONtraceptive Research and Development (CONRAD) consortium. We thank the members of the public/private Applied Molecular Pharmacology for Post-testicular Activity network for their continuous support and critical discussions on the GPX5 model. We wish to thank G. Grizard (Centre d'Etude et de Conservation des Oeufs et du Sperme — Centre Hospitalier Universitaire, Clermont Ferrand, France) for offering access to the computer-assisted sperm analysis facility. We are indebted to Felicity Vear (Institut National de la Recherche Agronomique, Clermont Ferrand, France) for English grammar and syntax corrections.

Received for publication February 17, 2009, and accepted in revised form April 15, 2009.


Address correspondence to: Joel R. Drevet, "Epididymis & Sperm Maturation," GReD, CNRS UMR 6247, INSERM U931, Clermont Université, 24 avenue des Landais, 63177 Aubière CEDEX, France. Phone: 33-4-73-40-74-13; Fax: 33-4-73-40-70-42; E-mail: joel.drevet@univ-bpclermont.fr.


1. Jones, R. 1998. Plasma membrane structure and remodelling during sperm maturation in the epididymis. *J. Reprod. Fertil. Suppl.* **53**:73–84.
2. Vernet, P., Aitken, R.J., and Drevet, J.R. 2004. Antioxidant strategies in the epididymis. *Mol. Cell Endocrinol.* **216**:31–39.
3. Cocuzza, M., Sikka, S.C., Athayde, K.S., and Agarwal, A. 2007. Clinical relevance of oxidative stress and sperm chromatin damage in male infertility: an evidence based analysis. *Int. Braz. J. Urol.* **33**:603–621.
4. Drevet, J.R. 2006. The antioxidant glutathione peroxidase family and spermatozoa: a complex story. *Mol. Cell. Endocrinol.* **250**:70–79.
5. Marchesi, D.E., and Feng, H.L. 2007. Sperm DNA integrity from sperm to egg. *J. Androl.* **28**:481–489.
6. Ghyselinck, N.B., et al. 1993. Structural organization and regulation of the gene for the androgen-dependent glutathione peroxidase-like protein specific to the mouse epididymis. *Mol. Endocrinol.* **7**:258–272.
7. Rejraji, H., Vernet, P., and Drevet, J.R. 2002. GPX5 is present in the mouse caput and cauda epididymidis lumen at three different locations. *Mol. Reprod. Dev.* **63**:96–103.
8. Vernet, P., Faure, J., Dufaure, J.P., and Drevet, J.R. 1997. Tissue and developmental distribution, dependence upon testicular factors and attachment to spermatozoa of GPx5, a murine epididymis-specific glutathione peroxidase. *Mol. Reprod. Dev.* **47**:87–98.
9. Dufaure, J.P., Lareyre, J.J., Schwaab, V., Mattei, M.G., and Drevet, J.R. 1996. Structural organization, chromosomal localization, expression and phylogenetic evaluation of mouse glutathione peroxidase encoding genes. *C. R. Acad. Sci. Paris.* **319**:559–568.
10. Schwaab, V., Faure, J., Dufaure, J.P., and Drevet, J.R. 1998. GPx3: the plasma-type glutathione peroxidase is expressed under androgenic control in the mouse epididymis and vas deferens. *Mol. Reprod. Dev.* **51**:362–372.
11. Delaunay, A., Pflieger, D., Barrault, M.B., Vinh, J., and Toledano, M.B. 2002. A thiol peroxidase is an $H_2O_2$ receptor and redox-transducer in gene activation. *Cell.* **111**:471–481.
12. Pfeifer, H., et al. 2001. Identification of a specific sperm nuclei selenoenzyme necessary for protamine thiol cross-linking during sperm maturation. *FASEB J.* **15**:1236–1238.
13. Conrad, M., et al. 2005. The nuclear form of phospholipid hydroperoxide glutathione peroxidase is a protein thiol peroxidase contributing to sperm chromatin stability. *Mol. Cell. Biol.* **25**:7637–7644.
14. Pushpa-Rekha, T.R., Burdsall, A.L., Oleksa, L.M., Chisolm, G.M., and Driscoll, D.M. 1995. Rat phospholipid-hydroperoxide glutathione peroxidase. cDNA cloning and identification of multiple transcription and translation start sites. *J. Biol. Chem.* **270**:26993–26999.
15. de Lamirande, E., and Gagnon, C. 1995. Impact of reactive oxygen species on spermatozoa: a balancing act between beneficial and detrimental effects. *Hum. Reprod.* **10**:15–21.
16. Bedford, J.M., and Calvin, H.I. 1974. The occurrence and possible functional significance of S-S- cross-links in sperm heads, with particular reference to eutherian mammals. *J. Exp. Zool.* **188**:137–155.
17. Bedford, J.M., and Calvin, H.J. 1974. Changes in -S-S-linked structures of the sperm tail during epididymal maturation with comparative observations in sub-mammalian species. *J. Exp. Zool.* **187**:181–204.
18. Calvin, H.I., and Bedford, J.M. 1971. Formation of disulfide bonds in the nucleus and accessory structures of mammalian spermatozoa during maturation in the epididymis. *J. Reprod. Fertil. Suppl.* **13**:65–75.
19. Calvin, H.I., Yu, C.C., and Bedford, J.M. 1973. Effects of epididymal maturation, zinc (II), and copper (II) on the reactive sulfhydryl content of structural elements in rat spermatozoa. *Exp. Cell Res.* **81**:333–341.
20. Cornwall, G.A., Vindivich, D., Tillman, S., and Chang, T.S.K. 1989. The effect of sulfhydryl oxidation on the morphology of immature hamster epididymal spermatozoa induced to acquire motility in vitro. *Biol. Reprod.* **39**:141–145.
21. Roveri, A., Ursini, F., Flohé, L., and Maiorino, M. 2001. PHGPx and spermatogenesis. *Biofactors.* **14**:213–222.
22. Seligman, J., Kosower, N.S., Weissenberg, R., and Shalgi, R. 1994. Thiol-disulfide status of human sperm proteins. *J. Reprod. Fertil.* **101**:435–454.
23. Seligman, J., Newton, G.L., Fahey, R.C., Shalgi, R., and Kosower, N.S. 2005. Nonprotein thiols and disulfides in rat epididymal spermatozoa and epididymal fluid: role of gamma-glutamyl-transpeptidase in sperm maturation. *J. Androl.* **26**:629–640.
24. Shalgi, R., Seligman, J., and Kosover, N.S. 1989. Dynamics of the thiol status of rat spermatozoa during maturation: analysis with the fluorescent labelling agent monobromobimane. *Biol. Reprod.* **40**:1037–1045.
25. Yanagimachi, R. 1994. Mammalian fertilization. In *The physiology of reproduction*. K. Knobil and J.D. Neill, editors. Raven Press. New York, New York, USA. 189–317.
26. Galantino-Homer, H.L., Visconti, P.E., and Kopf, G.S. 1997. Regulation of protein tyrosine phosphorylation during bovine sperm capacitation by a cyclic adenosine 3′5′-monophosphate-dependent pathway. *Biol. Reprod.* **56**:707–719.
27. Lewis, S.E., and Aitken, R.J. 2005. DNA damage to spermatozoa has impacts on fertilization and pregnancy. *Cell Tissue Res.* **322**:33–41.
28. de Lamirande, E., and O'Flaherty, C. 2008. Sperm activation: role of reactive oxygen species and kinases. *Biochim. Biophys. Acta.* **1784**:106–115.
29. Vernet, P., Rigaudiere, N., Ghyselinck, N.B., Dufaure, J.P., and Drevet, J.R. 1996. *In vitro* expression of a mouse tissue specific glutathione-peroxidase-like protein lacking the selenocysteine can protect stably transfected mammalian cells against oxidative damage. *Biochem. Cell Biol.* **74**:125–131.
30. Vernet, P., et al. 1999. Selenium-independent epididymis-restricted glutathione peroxidase 5 protein (GPx5) can back-up failing Se-dependent GPxs in mice subjected to selenium-deficiency. *Mol. Reprod. Dev.* **54**:362–370.
31. Zhang, T., et al. 2008. *gpx5*, the selenium-independent glutathione peroxidase-encoding single copy gene is differentially expressed in the mouse epididymis. *Reprod. Fertil. Dev.* **20**:615–625.
32. Balhorn, R., Corzett, M., Mazrimas, J., and Watkins, B. 2001. Identification of bull protamine disulfides. *Biochemistry.* **30**:175–181.
33. Rousseaux, J., and Rousseaux-Prevost, R. 1995. Molecular localization of free thiols in human sperm chromatin. *Biol. Reprod.* **52**:1066–1072.
34. de Haan, J.B., et al. 1998. Mice with a homozygous

null mutation for the most abundant glutathione peroxidase Gpx1, show increased susceptibility to the oxidative stress-inducing agents paraquat and hydrogen peroxide. *J. Biol. Chem.* **273**:22528–22536.
35. Imai, H., et al. 2003. Early embryonic lethality caused by targeted disruption of the mouse PHGPx gene. *Biochem. Biophys. Res. Com.* **305**:278–286.
36. Yant, L.J., et al. 2003. The selenoprotein GPx4 is essential for mouse development and protects from radiation and oxidative damage insults. *Free Radic. Biol. Med.* **34**:496–502.
37. Perl, A., et al. 2006. Transaldolase is essential for maintenace of the mitochondrial transmembrane potential and fertility of spermatozoa. *Proc. Natl. Acad. Sci. U. S. A.* **103**:14813–14818.
38. Kodama, H., Yamaguchi, R., Fukuda, J., Kasai, H., and Tanaka, T. 1997. Increased oxidative deoxyribonucleic acid damage in the spermatozoa of infertile male patients. *Fertil. Steril.* **68**:519–524.
39. Evenson, D.P., et al. 1999. Utility of the sperm chromatin assay as a diagnostic and prognostic tool in the human fertility clinic. *Hum. Reprod.* **14**:1039–1049.
40. O'Brien, J., and Zini, A. 2005. Sperm DNA integrity and male infertility. *Urology.* **65**:16–22.
41. Spano, M., et al. 2000. Sperm chromatin damage impairs human fertility. *Fertil. Steril.* **73**:43–50.
42. Zini, A., Bielecki, R., Phang, D., and Zenzes, M.T. 2001. Correlations between two markers of sperm DNA integrity, DNA denaturation and DNA fragmentation, in fertile and infertile men. *Fertil. Steril.* **75**:674–677.
43. Zini, A., and Libman, J. 2006. Sperm DNA damage: clinical significance in the era of assisted reproduction. *CMAJ.* **175**:495–500.
44. Tesarik, J., Greco, E., and Mendoza, C. 2004. Late, but not early, paternal effect on human embryo development is related to sperm DNA fragmentation. *Hum. Reprod.* **19**:611–615.
45. Tesarik, J., Mendoza-Tesarik, R., and Mendoza, C. 2006. Sperm nuclear DNA damage: update on the mechanism, diagnosis and treatment. *Reprod. Biomed. Online.* **12**:715–721.
46. Maiorino, M., et al. 1995. Probing the presumed catalytic triad of selenium-containing peroxidases by mutational analysis of phospholipid hydroperoxide glutathione peroxidase (PHGPx). *Biol. Chem. Hoppe Seyler.* **376**:651–660.
47. Agarwal, A., and Said, T.M. 2005. Oxidative stress, DNA damage and apoptosis in male infertility: a clinical approach. *BJU International.* **95**:503–507.
48. Said, T., Paasch, U., Glander, H., and Agarwal, A. 2004. Role of caspases in male infertility. *Hum. Reprod. Update.* **10**:39–51.
49. Vicari, E., La Vignera, S., Castiglione, R., and Calogero, A.E. 2006. Sperm parameter abnormalities, low seminal fructose and reactive oxygen species overproduction do not discriminate patients with unilateral or bilateral post-infectious inflammatory prostato-vesiculo-epididymitis. *J. Endocrinol. Invest.* **29**:18–25.
50. Vernet, P., Fulton, N., Wallace, C., and Aitken, R.J. 2001. Analysis of reactive oxygen species generating systems in rat epididymal spermatozoa. *Biol. Reprod.* **65**:1102–1113.
51. Koppers, A.J., de Iuliis, G.N., Finnie, J.M., McLaghlin, E.A., and Aitken, R.J. 2008. Significance of mitochondrial reactive oxygen species in the generation of oxidative stress in spermatozoa. *J. Clin. Endocrinol. Metab.* **93**:3199–3207.
52. Weir, C.P., and Robaire, B. 2007. Spermatozoa have decreased antioxidant enzymatic capacity and increased reactive oxygen species production during aging in the brown Norway rat. *J. Androl.* **28**:229–240.
53. Barouki, R. 2006. Ageing, free radicals and cellular stress. *Med. Sci. (Paris).* **22**:266–272.
54. Aitken, R.J., De Iuliis, G.N., and McLachlan, R.I. 2008. Biological and clinical significance of DNA damage in the male germ line. *Int. J. Androl.* **32**:46–56.
55. Fernandez, J.L., et al. 2003. The sperm chromatin dispersion test: a simple method for the determination of sperm DNA fragmentation. *J. Androl.* **24**:59–66.